Forschungszentrum Karlsruhe

in der Helmholtz-Gemeinschaft

Wissenschaftliche Berichte

FZKA 6770

Actinide Migration Experiment in the HRL ÄSPÖ, Sweden: Results of Laboratory and In Situ Experiments (Part II)

Jürgen Römer, Bernhard Kienzler, Peter Vejmelka,
Eva Soballa, Annegret Görtzen, Markus Fuß

Institut für Nukleare Entsorgung

Forschungszentrum Karlsruhe GmbH, Karlsruhe

2002

Actiniden Migration Experiment im Untertagelabor ÄSPÖ, Schweden: Ergebnisse von Labor und In Situ Experimenten (Teil II)

Zusammenfassung

Es werden die Ergebnisse von Migrationsexperimenten in Bohrkernen dargestellt, die im Labor und in der CHEMLAB 2 Sonde unter in-situ Bedingungen am Äspö HRL stattfanden. Die Bohrkerne für beide Experimente wurden unter gleichen Bedingungen präpariert und zeigten ähnliche hydraulische Eigenschaften. Als radioaktiver Indikator wurden die Aktiniden Am(III), Pu(IV) und Np(V) benutzt. Der Np-Durchbruch war nicht verzögert im Vergleich zu einem inerten HTO Indikator. Der Wiedererhalt an Np lag unter 40%. Am und Pu ließen sich nicht vom Bohrkern eluieren. Es konnte nur eine obere Grenze für den Rückhaltungsfaktor von 135 abgeschätzt werden. Für nachfolgende Untersuchungen wurde der Bohrkern in dünne Scheiben senkrecht zur Achse zerschnitten und diese sowie das aufgefangene Sägemehl chemisch und radiochemisch analysiert. Optische Bilder der Scheiben zeigten die Geometrie des Fließpfades über die Länge des Kerns. Autoradiographiebilder der Scheiben ergaben ein ähnliche Verteilung beim Am und Np. Über eine TTA-Extraktion des Np von einigen Scheiben konnte gezeigt werden, dass Np(V) reduziert wurde und im vierwertigen Zustand zurückgehalten wurde. Im Labor- sowie im in-situ-Experiment konnten bei der Sorption keine unterschiedlichen Prozesse oder Bedingungen entlang des Fließweges nachgewiesen werden, sondern es war eine Frage der Geometrie und der verfügbaren Fläche.

Abstract

Results of migration experiments performed in laboratory and in the CHEMLAB 2 probe under in-situ conditions at Äspö HRL with fractured drill cores are presented. Drill cores for both experiments are prepared by the same method and provide similar hydraulic properties. As tracers, the actinides Am(III), Pu(IV) and Np(V) are applied. Breakthrough of Np is found to be unretarted in comparison to inert HTO tracer. Recovery of Np amounts to less than 40%. Am and Pu are not eluted from the cores. Lower limits of the retardation factors of 135 are calculated for both Am and Pu. Post mortem investigations of the fractured cores are performed by cutting perpendicular to the cylinder axis and subsequent chemical and radio-chemical analysis of abraded material and slices. Imaging of the slices reveals the geometry of the flow path. α-radiography of the slices shows similar distribution patterns of Np and Am. By TTA extraction of Np from some slices, it is shown that Np(V) undergoes reduction and is mostly retained in the tetravalent state. In the laboratory and in the in-situ experiment sorption is not primarily attributed to different sorption processes or properties along the flow path, but more to its local geometric properties and the available surface areas.

CONTENT

TABLES

FIGURES

1   Background and Objectives

The Äspö Hard Rock Laboratory (HRL) was established in Sweden in a granite rock forma-tion for in-situ testing of disposal techniques and for investigations concerning migration and retention of radionuclides (Bäckblom, 1991). Groundwater flow through fractures in granite host rocks may cause migration of radionuclides from the repository. Within the scope of a bilateral cooperation between Svensk Kärnbränslehantering AB (SKB) and Forschungszen-trum Karlsruhe, Institut für Nukleare Entsorgung (FZK-INE), actinide migration experiments with Pu, Am, and Np are conducted at the Äspö Hard Rock Laboratory. Batch experiments provided information on the sorption behavior of different solids present at Äspö HRL. At first, migration experiments were performed in laboratory at FZK-INE, afterwards, the same ex-periments were repeated at Äspö HRL. To guarantee most realistic conditions, the experi-ments are performed in the CHEMLAB 2 probe (Jansson, 1997).

Previous reports summarized the results of batch experiments and laboratory tests with core #1 as well as results of the first in-situ experiment (Vejmelka et al., 2000; Vejmelka et al., 2001, Kienzler et al 2002).

2   Materials

2.1   Groundwater

For laboratory investigations, Äspö groundwater was used, which was extracted from the drill hole SA 2600, whereas in the in-situ experiment natural groundwater is present in the CHEMLAB 2 borehole KJ0044F01. Both compositions are given in Kienzler et al 2002. Both waters differ in the measured concentrations by about 30-60%. Fe could not be measured in the groundwater used in laboratory (SA 2600). Fe had been precipitated during the transport to Germany.

The laboratory experiments were performed in a glove box under a 99% Ar, 1% CO_2 atmos-phere. At Äspö HRL under the conditions prevailing in the CHEMLAB drill hole, the CO_2 par-tial pressure was computed to be log p_{CO2} = -2.6 which was only slightly different as in labo-ratory (log p_{CO2} = -2.0).

2.2   Fracture Surfaces

Migration experiments in laboratory and in CHEMLAB 2 required fractured core samples. The material covering the fracture surfaces was analyzed by scanning electron microprobe (SEM). Results of element mapping of granite and the altered material in a fracture is shown

in Fig. 1. In unaltered granite, SiO_2 dominates, whereas in the altered material other main components such as, Al, K, Mg and Ca containing phases are present. Iron oxide containing particles showed Fe-concentrations of a factor of 200 above the surrounding rock. X-ray diffraction pattern showed the mineral chlorite as a main constituent.
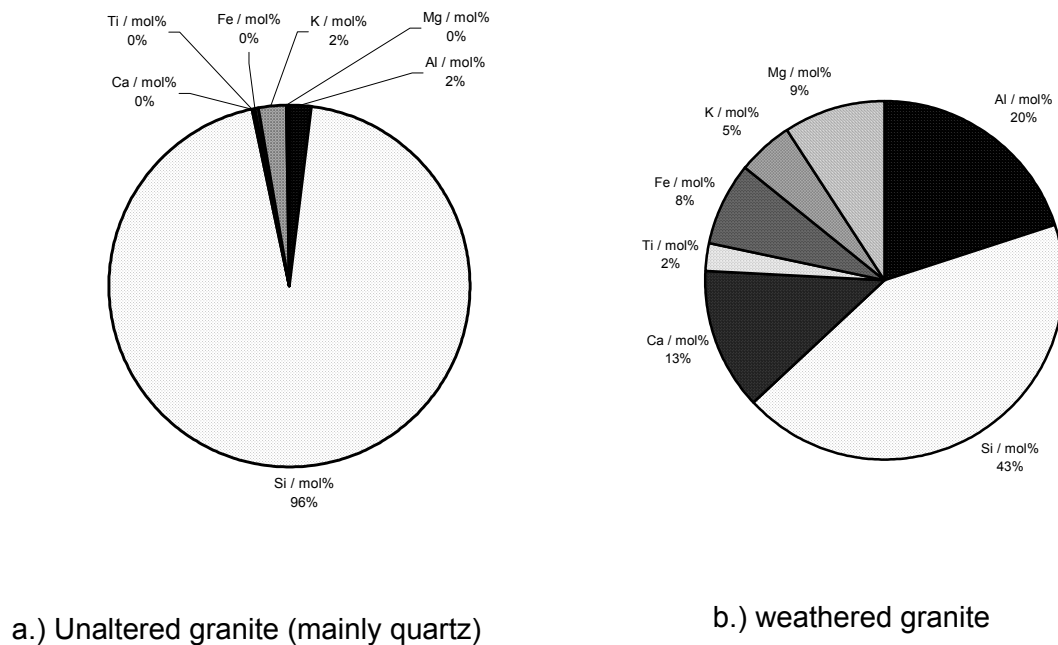

a.) Unaltered granite (mainly quartz)

b.) weathered granite

Fig. 2-1   Element mapping of granite and altered material within a fracture

2.3 Radionuclides

For in-situ and laboratory migration experiments, actinide tracer cocktails of the long-lived isotopes [244]Pu(IV), [243]Am(III), and [237]Np(V) were prepared according to the maximum solubilities of these actinides in SA 2600 groundwater from Äspö HRL. Np, Pu and Am were added to the groundwater leading to concentrations as follows: [244]Pu approx. $1x10^{-8}$ mol·dm^{-3}, [243]Am approx. $1x10^{-6}$ mol·dm^{-3} in laboratory, and $1x10^{-8}$ mol·dm^{-3} for the in-situ experiment at Äspö, and [237]Np approx. $1x10^{-5}$ mol·dm^{-3}. Total α-activity of the CHEMLAB cocktail amounted to $1.8x10^4$ Bq·dm^{-3}. For determination of hydraulic properties of fracture and monitoring of the in-situ experiments HTO tracer was added.

3   Migration experiments

The two cores used in laboratory and in the CHEMLAB 2 probe showed partly open fractures at both ends. To some extent, the fractures were filled with fracture filling material; the cores

stuck together during preparation. Both cores were placed into cylindrical stainless steel sleeves. The design of these autoclaves is shown in Kienzler (2002). The periphery between cores and steel was filled with epoxy resin. Top and bottom ends were closed with acrylic glass covers. Sealing between the top / bottom ends and the stainless steel sleeve was achieved by O-rings. The lids were provided with fittings for feeding and extracting the groundwater. Tightness of the autoclaves was tested in subsequent laboratory experiments, indicating a leak tightness up to 60 bar groundwater pressure. The fluid pressure in CHEM-LAB 2 is about 27 bar.

Migration experiments were performed in laboratory and in the CHEMLAB 2 probe following the same experimental scheme. The arrangements in the Äspö HRL are shown in Kienzler et al (2002). In CHEMLAB 2 and in laboratory, the same injection procedure was applied. The laboratory core #4 was used for 3 subsequent experiments, and one experiment was pre-formed with core #2. In each experiment, 14000 µL of cocktail were injected at constant flow rate of 0.3 mL/h. Breakthrough of HTO and actinides was recorded by collecting about 40 drops per sample (0.96 mL). These samples were analyzed by LSC and by ICP-MS, respectively.

After termination of the experiments, the cores were cut perpendicular to the cylinder axis. Thickness of slices was 4 mm, thickness of the diamond blade was 0.7 mm. Abraded material was dissolved and analyzed with respect to the injected actinides and natural uranium and thorium by means of ICP-MS. The slices were scanned by means of an optical scanner using a resolution of 600x600 pixel per inch. The radioactivity retained in each slice was measured by means of spatial resolved radiography (Cyclone Phosphor Scanner, Packard BioScience, Dreieich, Germany) at the same resolution. By means of γ-scanning (γ-detector by Canberra, Eurisys GmbH, Germany) for the 74.4 keV lines of ^{243}Am and the 312 keV line of ^{233}Pa daughter of ^{237}Np. In order to evaluate the efficiency of these measurements, the background concentration of radionuclides such as natural U and Th were measured in the abraded material by ICP-MS and presented in Tab. 3-1.

Tab. 3-1 Natural U and Th concentrations in the solids

	Thorium	Uranium
Core #2	8600 $\pm$ 2560 ng/g (37 $\pm$ 11 nmol/g) 0.35 Bq/g	3000 $\pm$ 70 ng/g (12.5 nmol/g) 0.38 Bq/g
Core #4	52000 $\pm$ 9000 ng/g (220 $\pm$ 30 nmol/g) 2 Bq/g	8600 ng/g $\pm$ 10% (36 nmol/g) 1 Bq/g

Concentrations of Np and Am were determined by γ-counting as well as by ICP-MS measurement of the dissolved abraded material. Analyses of the redox state of retained Np were performed by dissolution of Np from sliced by HCl and subsequent TTA extraction.

4 Results and discussion

Hydraulic properties of the cores were determined from HTO breakthrough curves and are summarized in Tab. 4-1. Dispersion coefficient D of core #2 exceeded the value measured for core #4. For both cores, pore volumes and hydraulic properties were comparable.

Tab. 4-1 Hydraulic properties of laboratory core #4 and CHEMLAB core #2

		Core #4	Core #2
Origin		KA 2195 A02	KA 2195 A02
l	m	0.150	0.150
$\varnothing_{core}$	m	0.052	0.052
σ^2_t	-	1.09 ± 0.20	1.05 ± 0.32
D	m^2/s	$(1.1 \pm 0.2) \times 10^{-6}$	$(3.9 \pm 1.2) \times 10^{-6}$
α	m	0.082 ± 0.015	0.079 ± 0.024
Pore Volume	ml	1.90 ± 0.35	1.98 ± 0.59
	l:	Length	
	$\varnothing_{core}$	Diameter of the core	
	σ^2_t:	Variance	
	D:	Dispersion coefficient	
	α:	Dispersion length	

4.1 Breakthrough of actinides

Tab. 4-2 shows the schemes of the migration experiments under discussion. Three subsequent actinide experiments were performed with core #4 in laboratory injecting 14 mL of actinide cocktail. 82 mL of eluted water was collected in the first experiment, 56 mL and 132 mL were collected in the following runs, respectively. Only in the first experiment with core #4, an breakthrough of Np was observed. At the maximum the count rate was 36 Bq/mL (12 $\mu mol \cdot dm^{-3}$). In the following tests, Np was found in concentrations of 0.06 and 0.2 $\mu mol \cdot dm^{-3}$ close to the detection. Am and Pu were not detected in the eluated water. In order to monitor the breakthrough, HTO tracer was added to the cocktail in the 2nd and 3rd experiment. HTO was detected already in the first fraction. The maximum HTO concentrations occurred in the samples between 4.8 and 14.4 mL and 3.8 and 13.4 mL, respectively.

The same injection scheme was applied in CHEMLAB 2. The breakthrough of Np and HTO determined in the CHEMLAB and in laboratory experiment is presented in Fig. 2. The figure shows the Np injection curve, the measured ^{237}Np concentration and the HTO activity in the eluted samples after filtration by 450 nm filters. It is obvious that the breakthrough of Np follows the tendency of the HTO curve. In laboratory experiments as well as in the in-situ experiment, breakthrough of Np is observed to be unretarted compared to the inert HTO tracer.

Recovery of Np in the first core #4 experiment was about 26 %, whereas in the CHEMLAB experiment 40 % of Np were recovered. Am and Pu concentrations could not be detected in the eluted samples of all experiments under discussion.

Tab. 4-2 Schemes of core #2 and core #4 experiments

		Core #2 CHEMLAB	Core #4
Injection of cocktail	14 mL	X	X
Flow rate	0.3 mL/h	X	X
Eluted volume (1)	mL	43.8	82.5
(2)	mL		40.8
(3)	mL		132.5

From core #4 experiments, a lower limit for the retardation factors of Am and Pu can be estimated. By comparing the pore volume to the total eluted volume of the 3 consecutive experiments $R_s = 135$ is obtained.
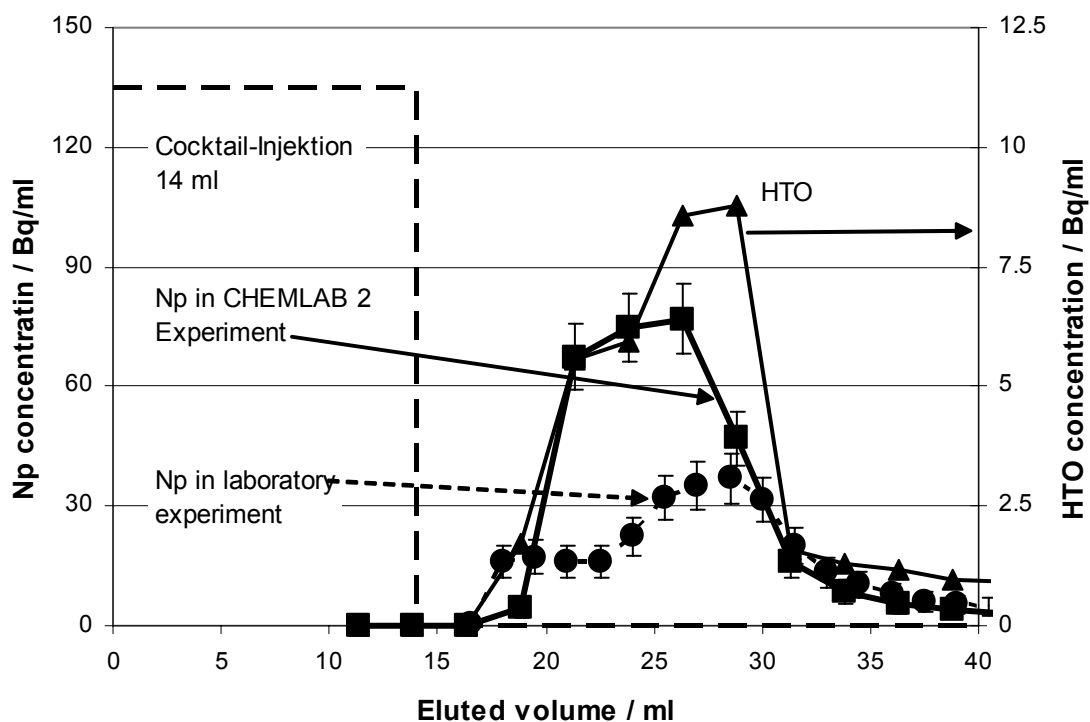

Fig. 4-1   Measured breakthrough of Np in core #2 and #4 and HTO in core #2

squares: CHEMLAB2 experiment, diamonds: laboratory experiment

5

4.2 Post mortem investigations of the fractures

Core # 2 and #4 show partly open fractures at both ends. Fracture filling material is coloured differently in comparison to the surrounding granite. Although core # 2 shows a significant pressure rise during the experiment, we tried to fill the cavities and pores of core #2 with a fluorescent colored epoxy resin in order to mark the flow path. After a drying procedure, the resin was pumped into the core. Core #2 was cut into 31 slices (perpendicular to the cylinder axis), each slice surface was inspected for the fluorescent resin. Only at very small parts of the surface of a few slices the resin could be detected by ultraviolet light. The cross-sections of the flow path is found to be extremely small, the diameters are significantly less than one mm. Only in one end of core #2 (slice #23, #24, #25) the fluorescent resin is present in the periphery. Because no radioactivity was measured in these parts of the slices, it can be assumed that some small-sized fractures were produced during the resin injection procedure. Images of some slices are shown in Fig. 4-2. The yellow color of slice #24 represents the fluorescent resin; the grey-green band represents fracture filling material. The complete set of images is shown in appendix A. In Fig. 4-2, the variation of the size, geometry and orientation of the fracture/fracture filling material along core #2is obvious.

A selection of slices from core #2 (#1, #3, #5, #11, #16, #19, #22, #25, #30) are examined by α-autoradiography. A micro imager (Zinsser Analytic GmbH) was used. The instrument required samples of 24 mm x 32mm, maximum. For this reason, the slices had to be cut into appropriate sizes. The area of the visible fracture was selected. Fig. 4-3 shows an optical image of slice #1 and #3 overlayed by the corresponding images containing the autoradiographic information. In both slices, the adsorbed radioactivity is located only in a small region of the fracture. The other images are shown in the appendix. In some of the radiographic images no radioactive spots could be detected. An explanation could be that only parts of the slices were analyzed by the Zinsser micro imager.

Fig. 4-2   Slice #1, #16 and slice #24 of core #2 (colored resin in the periphery)
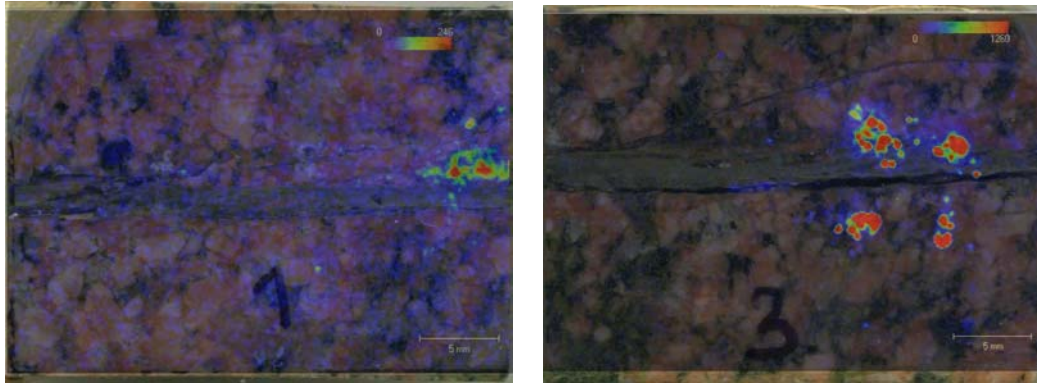
Fig. 4-3   Overlayed autoradiography with optical image of slice #1 and #3 (core #2)

Optical image of slice #2   relative distribution of α-activity of slice #2   overlayed image
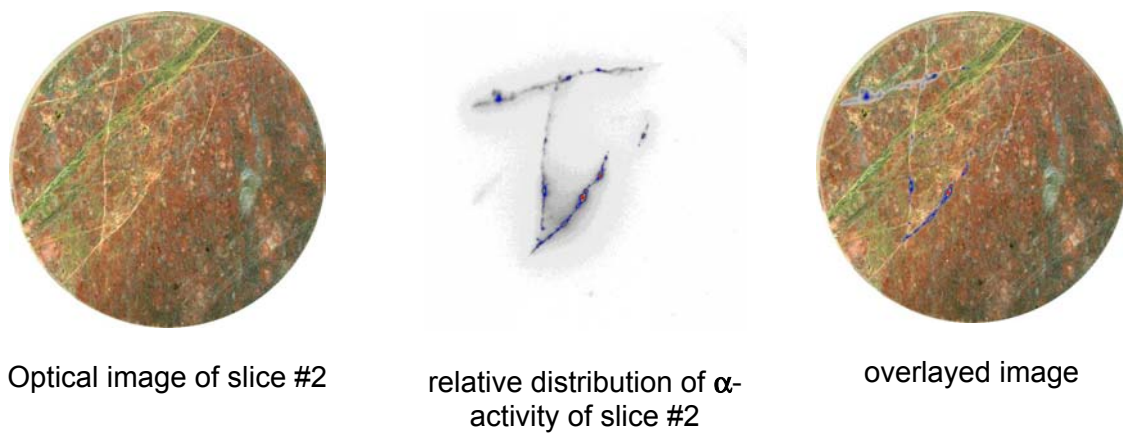
Fig. 4-4   Images of optical scans, distribution of α-activity in slice #2 and overlay image obtained by cutting the core #4 (perpendicular to the cylinder axis)

The core #4, which was used in the laboratory, required a high pressure load during the flow through experiment. Therefore, no resin was injected. The core was cut without fluorescent resin into 27 slices and the actinide concentrations retained in each slice were measured by γ-scanning and by ICP-MS measurement of the dissolved material abraded during the cutting.
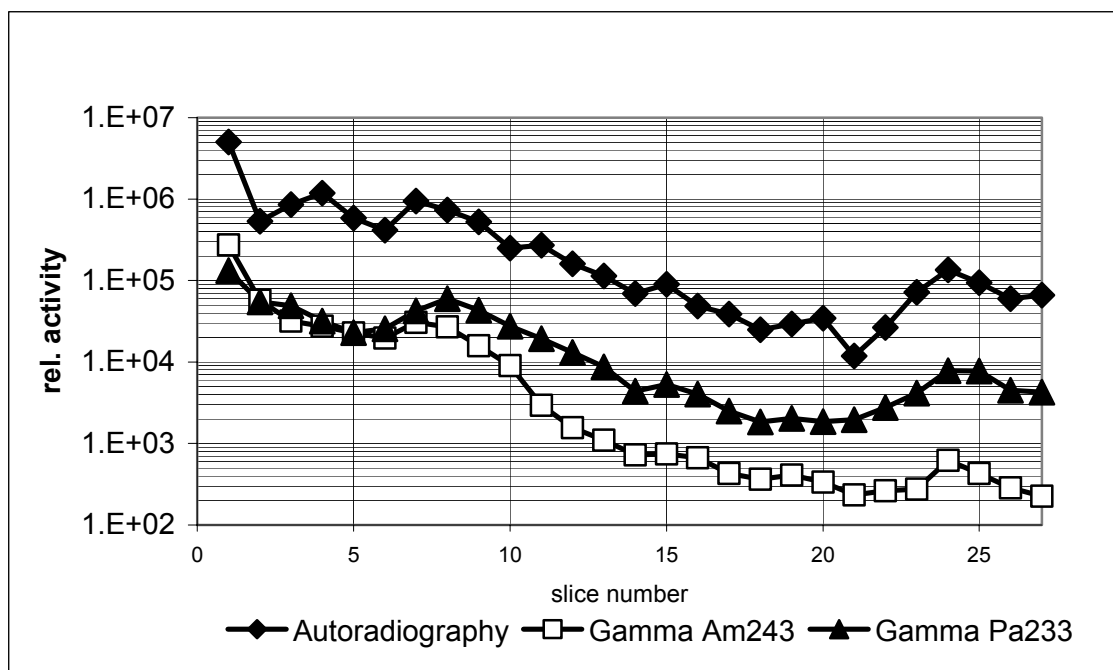
Fig. 4-5   Comparison of the autoradiography data against γ-scans of Am243 and Pa233

To avoid cutting of slices, a new autoradiography instrument using α- and β-sensitive sheets was applied (dimension 12.5 cm x 25.2 cm). By this method, whole slices can be analyzed and optical and autoradiographic images of the same resolution are produced. Fig. 4-4 shows for example slice #2 (core #4): left hand side an optical scan, in the middle the distribution of α-activity and at the right hand side the overlayed image of optical and α-autoradiographic information. Again, the adsorbed activity is not correlated with the size and the location of the visible fracture filling material. α-distribution corresponds with fine cracks. The origin of these cracks is not yet investigated. All pictures combining optical and radiographic scans are presented in appendix C. The red color which is to be seen in the autoradiographic scans presents the highest α-activity. A comparison between the pictures shows, that the adsorbed nuclides are not correlated with the fracture filling material.

The relative activity of the slice surfaces can be determined by integration of the autoradiography data. Fig. 4-5 shows a comparison of the relative α-activity against the γ-activity for the slices of core #4. A good correlation exists between the autoradiography data, mainly determined by ^{243}Am activity, and the corresponding γ-dose.

For interpretation and comparison of the data obtained for core #4, one has to keep in mind, that 3 distinct experiments were performed with this core. The recovery measured for ^{237}Np varied between 40% in the CHEMLAB experiment and 26% in the first and zero in the following two laboratory tests. pH in the eluted samples was about pH 7, Eh of the eluted samples ranged from +30 to -60 mV.

Fig. 4-6 reveals measured Np distribution in cores #2 and #4 obtained by analysis of dissolved abraded material. In Fig. 8, data obtained by both analytical methods are presented for core #4. Results obtained by both methods are in reasonable agreement. Due to the three different experiments, Fig. 4-7 shows a higher Np content in the abraded material of

core #4 than for core #2. The distribution of Np in core #4 shows the highest values directly at the injection (distance 0 to 5 mm), a first peak at a distance between 30 and 40 mm and a 3rd less pronounced peak between 104 and 118 mm. All these peaks are indicated by several measurements of abraded material as well as by γ-counting of ^{233}Pa. The three peaks are also found in the ^{243}Am distribution at almost the same locations. In the CHEMLAB core #2, a broad Np distribution between 50 and 112 mm was recorded.
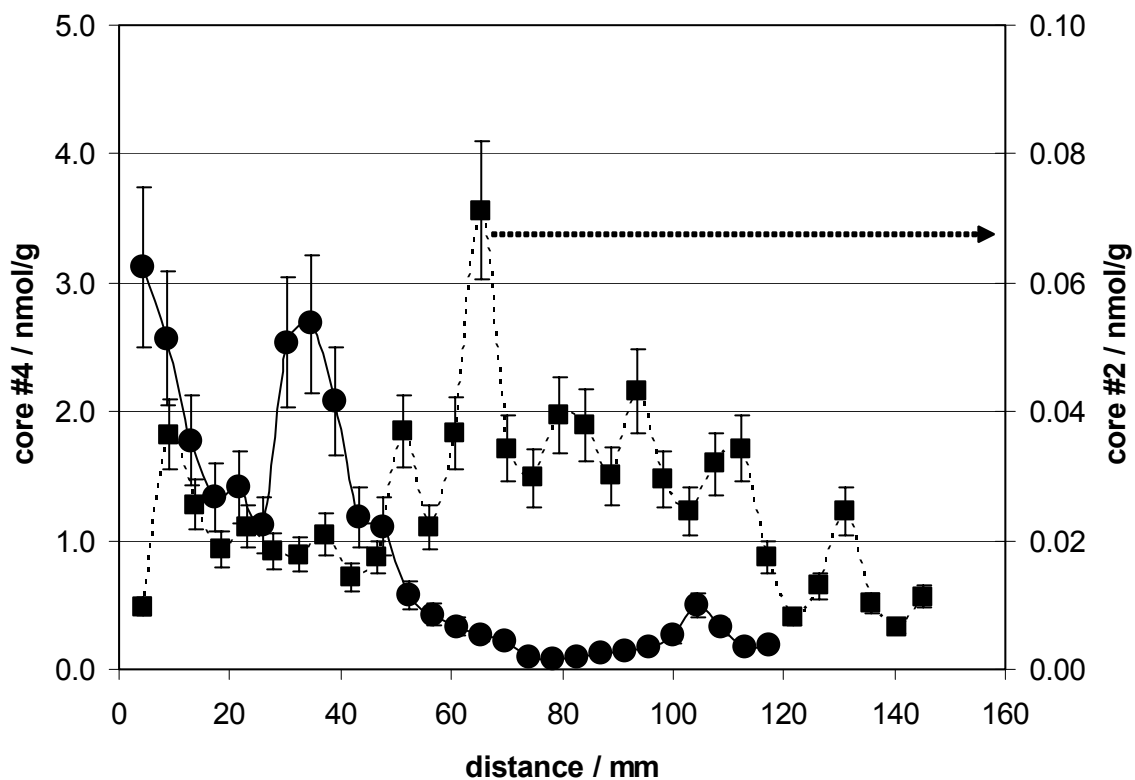
Fig. 4-6   Measured Np distribution in cores #2 and #4 by ICP-MS analysis of dissolved abraded material

circles: core #4, squares: core #2
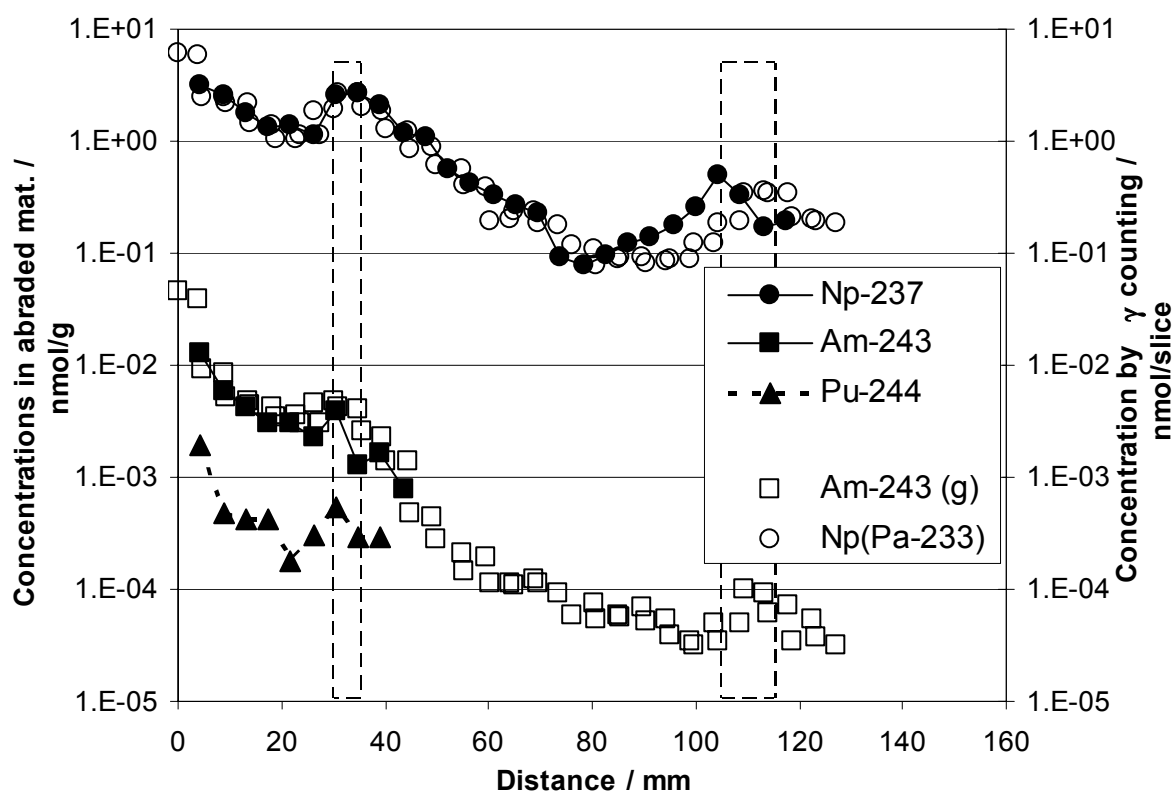
Fig. 4-7   Comparison of sorbed actinides measured by γ-scanning and by ICP-MS measurement of dissolved abraded material

In core #4, highest ^{244}Pu concentration could be detected at zero distance. At the distance of 30 mm, a single measurement surmounts the concentrations found in adjacent slices. At distances greater than 40 mm, ^{244}Pu concentration in the abraded material was below detection limit. For core #2, ^{243}Am and ^{244}Pu was everywhere below the detection limit of 0.3 pmol/g (0.07 ng/g).

Slices of both cores were analyzed by means of α-radiography and the α-distribution was compared with optical scans of the slices. Fig. 5 shows the results. In both cores complicated distributions of retained α-emitters were found. At the maximum, Np activity in core #2 accounts to 5 Bq/g and to 20 Bq/g for core #4. The spatial patterns obtained by α-radiography were not necessarily correlated with fracture filling material which could be discriminated from granite by its color. The spatial resolution of α-radiography is constrained by the natural radioactivity arising from the U and Th content of granite. These elements are in equilibrium with their decay chain, including β-emitters. For both cores, the total number of Np decays was in the same range as the number of α-decays produced by natural decay chains of U and Th.

5   Evaluation of sorbed actinides

From the investigation presented here, information on the retention mechanism can be obtained. In the cocktail injected into the cores, the actinides were present as Am(III), Pu(IV) and Np(V). Comparisons between the actinides show for core#4 that all actinides are retained in the same locations. Am(III) is the most stable redox state of this element. For this reason, one can assume that retention of Am does not depend on reduction/oxidation processes. The redox state of Np was analyzed in the 2nd and 8th slice. Np was dissolved with HCl and by TTA extraction Np(IV) was separated. As a result, it was found that more than 60% of Np was bound to the slices in the form of Np(IV). Np(V) in solutions, even at negative Eh (e.g. in the cocktail) remained as Np(V) for many month as long as no solids were present. This indicates that solid granite and/or fracture filling material catalyses reductive processes. Potential sites for reduction processes might be pyrite and Fe(II) containing clay minerals which are detected in the Äspö granite.

From Pourbaix diagrams of Pu (Fig. 5-1), one can assume that for measured pH = 7.0 and Eh values between -60 and +30 mV that Pu can exist as Pu(III) and Pu(IV). If Pu is reduced, sorption behavior as in the case of Am(III) can be expected. In the trivalent state, solubility limit of Pu should not play any role under these conditions.
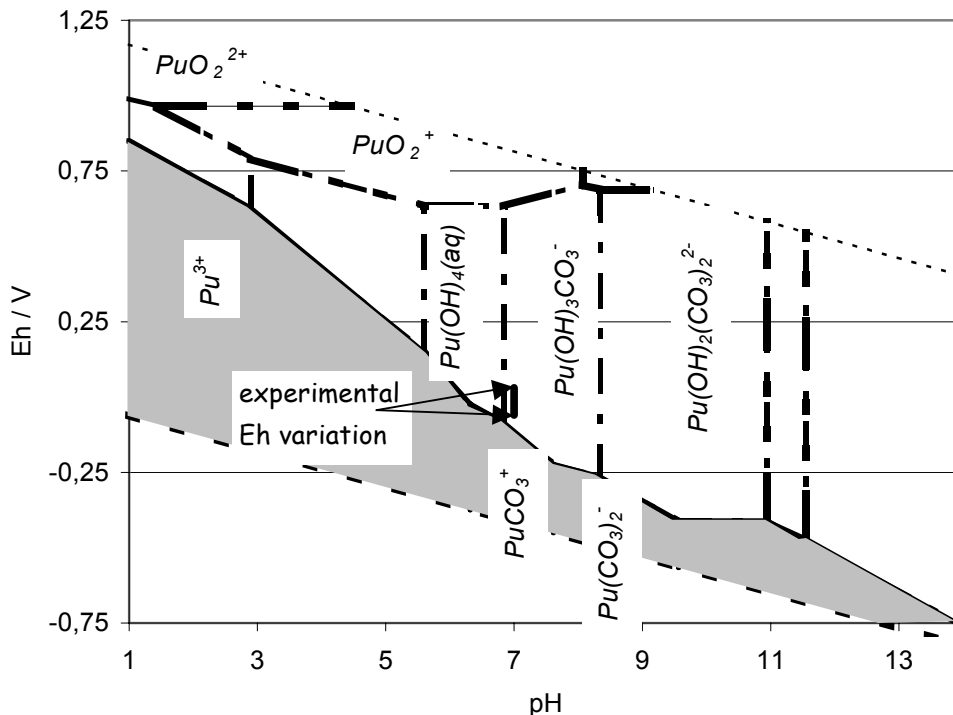

Fig. 5-1   pH-Eh diagram of dissolved Plutonium species in Äspö groundwater (log p CO_2 = -2.6) and Eh variation found in the experiments in laboratory and CHEMLAB

From these consideration, it can be concluded that the reason for the same spatial distribution patterns of Np and Am along the cores is not primarily attributed to different sorption processes, but more to the local geometric properties and the available surface areas along the flow paths.

Acknowledgment

6 Literatur

Bäckblom, G. 1991. The Äspö hard rock laboratory - a step towards the Swedish final repository for high-level radioactive waste. Tunnelling and Underground Space Technology 4, 463-467.

Bethke, C.M., 1999. The Geochemist's Workbench, Version 3. University of Illinois, USA.

Eliason, Th. 1993. Mineralogy, Geochemistry and Petrophysics of Red Coloured Granite Adjacent to Fractures. SKB Stockholm, TR 93-06.

Fuss, M., Fanghänel, E., Geckeis, H., Plaschke, M., Hauser, W., Görtzen, A., Römer, J., Spieler, K., Kim, J.I., 2001. Anwendung der Laserablation zur Radioanalytik. Annual GDCh Meeting, 23.-29.09.2001, Würzburg, Germany

Jansson, Mats, Erikson, Trygve E. 1998. CHEMLAB In-Situ Diffusion Experiments Using Radioactive Tracers, Radiochimica Acta 82, 153-156.

B. Kienzler, P. Vejmelka, J. Römer, E. Fanghänel, Swedish-German actinide migration experiment at Äspö hard rock laboratory, Cont. Hydrol. accepted for publication, Cont. Hydrology 2002.

Vejmelka, P., Fanghänel, Th., Kienzler, B., Korthaus, E., Römer, J., Schüßler, W., Artinger, R., 2000. Sorption and migration of radionuclides in granite (HRL ÄSPÖ, Sweden). Forschungszentrum Karlsruhe, FZKA 6488.

Vejmelka, P., Kienzler, B., Römer, J., Marquardt, Ch., Soballa, E., Geyer, F., Kisely, T., Heathman, D., 2001. Actinide migration experiment in the HRL ÄSPÖ, Sweden: Results of laboratory and in-situ experiments (Part I). Forschungszentrum Karlsruhe, FZKA 6652.

Appendix A   Optical images of core #2 (cutted perpenticular to the cylinder axis)
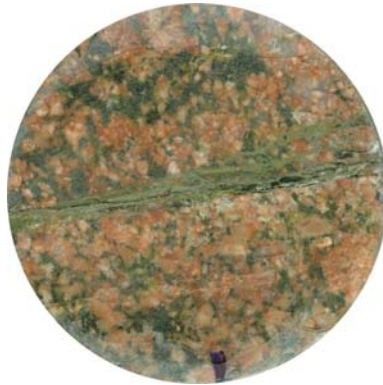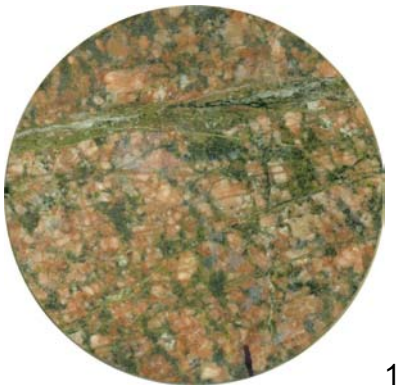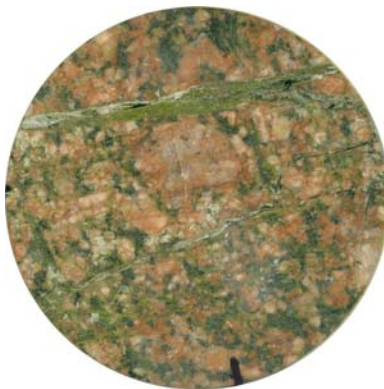

1

2

3

4

5

6

7

8

9

10

11

12

14

13

14

15

16

17

18

19

20

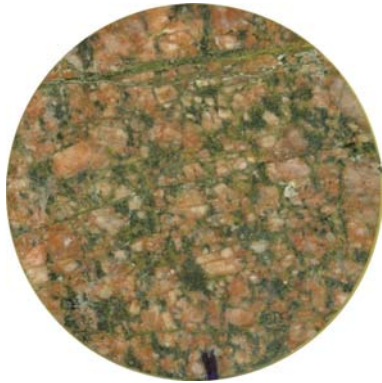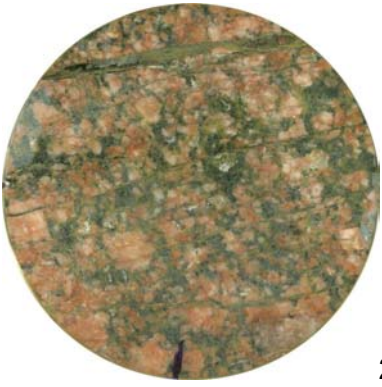21

22

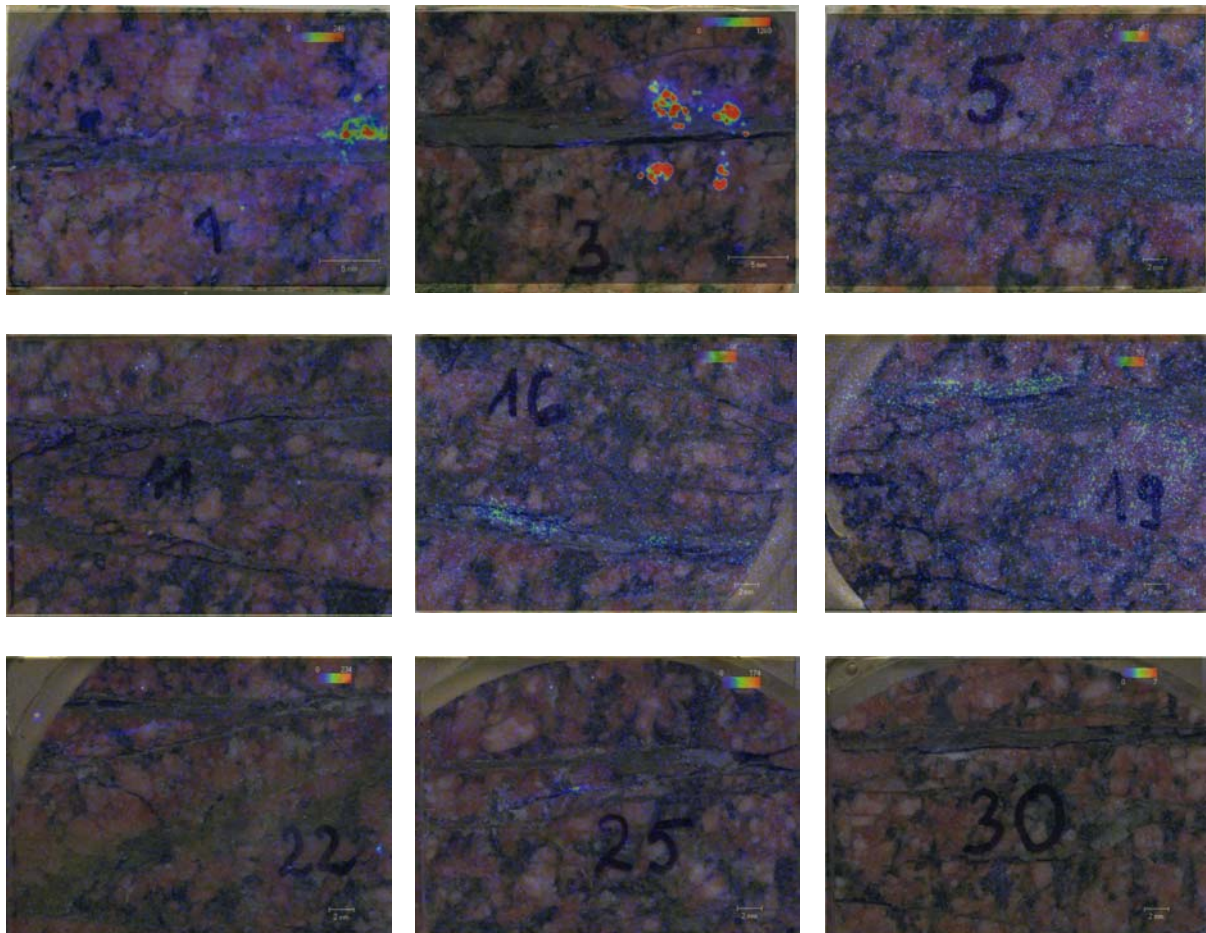23

24

25

26

27

28

29

30

31

Appendix B Optical images of slice #1, #3, #5, #11, #16, #19, #22, #25, #30 for core #2 overlayed with autoradiography of micro imager

Appendix C Combination of optical and radiographic scans